ABSTRACT

MARKS, WILLIAM LEWIS. Using L-Band Synthetic Aperture Radar to Estimate Basal Area and Biomass of Loblolly Pine Stands in the Neuse River Basin of North Carolina. (Under the direction of Dr. Siamak Khorram.)

The ability to use remote sensing techniques to estimate biophysical characteristics of forests, such as basal area and biomass, would allow surface maps of these properties to be generated over large areas that would normally be impractical to map using traditional field methods. The objective of this study was to assess the relationship of fully polarimetric L-band Synthetic Aperture Radar backscatter with *in situ* measurements of basal area and biomass of mature loblolly pine stands using simple linear regression. All stands were located in the Neuse River Basin of North Carolina in the Atlantic Coastal Plain. The sample set of field measurements was composed of 24 loblolly pine stands ranging from 10 to 50 m^2/ha of basal area and 65 to 265 t/ha of total biomass. Both natural and plantation stands were included. Correlation was assessed in three groups consisting of: [1] natural and plantation stands combined; [2] natural stands only; [3] and plantation stands only. R^2 values were calculated for each group based on 27 combinations of polarization (HH, VV, HV), pixel window size ($18m^2$, $30m^2$, and $42m^2$), and statistical operation (mean, minimum, and maximum backscatter value in each window).

Our results found relatively weak correlations between the backscatter data and the sample field measurements. HH polarization consistently displayed the lowest correlations while HV had the highest correlations in all groups for both basal area and biomass. The sample group

that included both the plantation stands and natural stands had the lowest correlations, with R^2 values of 0.2107 and 0.334 for basal area and biomass, respectively. When plantation stands were analyzed separately, correlation improved with R^2 values of 0.5251 for basal area and 0.4885 for biomass. Similarly, correlation improved when natural groups were analyzed separately. The highest correlation of the study was found for biomass in this group 0.6107 R^2). However, the basal area correlation was substantially lower with an R^2 of 0.3435.

The low correlations found in this study are likely due to the saturation of the L-band backscatter at basal area and biomass levels below those of the majority of our sample sites. The use of longer wavelength radar may be necessary to retain sensitivity in mature loblolly pine stands. This study has also displayed the value of stratifying forest stands into plantation and natural stands, as the different characteristics of each may degrade basal area and biomass estimation efforts when combined.

Using L-Band Synthetic Aperture Radar to Estimate Basal Area and Biomass of Loblolly Pine Stands in the Neuse River Basin of North Carolina

by
William Lewis Marks

A thesis submitted to the Graduate Faculty of
North Carolina State University
in partial fulfillment of the
requirements for the degree of
Master of Science

Natural Resources

Raleigh, North Carolina

2012

APPROVED BY:

_____	_____
Dr. Siamak Khorram Committee Chair	Dr. John Iiames
_____	
Dr. Heather Cheshire	

BIOGRAPHY

Will Marks has a BS in Geography from Southern Illinois University Edwardsville, and will hopefully soon have an MS in Natural Resources from North Carolina State University.

ACKNOWLEDGMENTS

To my committee members, Drs. Siamak Khorram, John Iiames, and Heather Cheshire, thank you very much for supporting me throughout my time at NC State. I have been given the opportunity to serve as a teaching assistant for all three professors in various classes. Without that source of funding and the associated tuition waiver, graduate school would not have been an option.

I would also like to extend my sincerest thanks to the members of the Landscape Characterization Branch at the US Environmental Protection Agency that provided guidance and expertise throughout this process. First and foremost, I would like to again thank Dr. John Iiames for being the driving force behind this project. Without John, I would have had neither a project nor funding. I would also like to thank Ross Lunetta for a great deal of technical input; Jayantha Ediriwickrema for his seemingly limitless knowledge of all things programming and his willingness to assist with my processing problems; Keith Endres for his assistance with field work and knack for tree identification; and finally, Megan Van Fossen for her consistent moral support and morning chats.

Thank you very much to Kate Farthing and Rachel Cook for the many hours spent tromping around in the woods of Eastern North Carolina while collecting measurements at sample sites. Without them, field measurements would have been physically impractical and most of all, far less entertaining.

TABLE OF CONTENTS

LIST OF FIGURES

LIST OF TABLES

1. Introduction

The Neuse River, located within the piedmont and coastal plain physiographic regions in North Carolina, has been identified as one of the most ecologically threatened rivers in the United States (American Rivers, 2007). The Neuse River has been suffering from degraded water quality since the 1970s, due in substantial part to excessive nitrogen (N) loadings which have led to eutrophication and episodic hypoxia (Paerl, et al., 1998; Whitall and Pearl, 2001). Modeling diffuse N sources, transport rates and delivery vectors to the Neuse River is an important objective for the United States Environmental Protection Agency's (USEPA) mission to better understand the location and magnitude of N sources across the Neuse River basin (Lunetta, et al., 2005). Overland flow may serve as a major source of N into the Neuse River tributaries due to the leaching of N from soil and impervious surface during hydrologic transportation events (Kruzic and Schroeder, 1990). The potential rate of N transportation has been shown to have a significant relationship to the rate of overland flow and an inverse relationship to surface roughness (Gilley et al., 2008). Overland flow rate is known to increase as vegetation stem density, basal area, biomass, and subsequently surface roughness, decreases (McEldowney, et al., 2002; USDA, 2001). The ability to model these vegetation parameters throughout the Neuse River watershed would potentially improve efforts to analyze N movement from nonpoint sources into the river.

The research presented here is a pilot study to assess the feasibility of using fully polarimetric NASA Uninhabited Aerial Vehicle Synthetic Aperture Radar (UAVSAR) L-

band data to characterize the basal area and biomass of mature loblolly pine (*Pinus taeda)* stands in the coastal plain of North Carolina. L-band radar was selected in favor of shorter wavelength C or X-band radar because research has shown that biomass sensitivity increases with wavelength (Imhoff, et. al., 1998). Both natural and plantation stands of loblolly pine were selected because they comprise the highest wood volume in the state (NCFS, 2010). *In situ* measurements were made at 24 sample sites throughout the study region. The stands range from 10 to 50 m^2/ha of basal area and 65 to 265 t/ha of total biomass. Though the small sample size precludes definitive conclusions, the outcome will help determine the feasibility of pursuing more comprehensive studies in the future. While airborne SAR has been used to varying degrees of success in many previous forest characterization studies, this is first research to specifically assess its feasibility under the described parameters.

2. Objectives

The primary objective of this study is to determine the feasibility of using the three polarizations (HH, VV, HV) of L-band SAR data to estimate basal area and biomass in mature loblolly pine in the North Carolina coastal plain based on three sets of field measurement samples: [1] natural and plantation stands combined (All Stands); [2] natural stands only (Natural Stands); [3] and plantation stands only (Plantation Stands). The relationship between backscatter and field measurements will be assessed using simple linear regression. The levels of correlation found in the different combinations of polarizations and

stand-type samples will help determine whether it will be worthwhile to pursue a more comprehensive study that includes a larger set of sample field measurements.

3. Background

Traditional methods of measuring basal area in forested areas require time and labor intensive ground-based surveys that are impractical to perform on a large scale. In addition to travel and navigation issues encountered for each site, collecting these data is also made difficult by the lack of accessibility to private land holdings. Thus, creating a state-wide database of basal area for all forested stands is infeasible using traditional methods. Basal area data collected remotely, whether by airplane or satellite, provides a more efficient alternative.

Remote sensing, in various forms, has been used in forest management applications for over 120 years, starting as early as 1887 when a German forester took aerial photos of a forest from a hot balloon (Franklin, 2001). World War I reinforced the usefulness of aerial photography in mapping and understanding problems on the ground. The advancements made in the techniques and technology during the first half of the century, driven mainly by the necessities of the two World Wars, rapidly accelerated the use of remote sensing in vegetation and forest management applications during the post-WWII years. As early as 1956, color-infrared film was being used in crop studies and by1960, the first meteorological satellite was launched. TIROS-1 served as the predecessor to the first multi-spectral imaging

satellite designed for land-monitoring, LANDSAT-1, launched1 in 1972 (Campbell, 2007). Multi-spectral and hyper-spectral imaging has since been used extensively in forest measurement applications. The post-War years also saw the introduction of radar as a useful tool for civilian vegetation and forest studies.

3.1 Radar

The earliest radar systems were developed in the 1920s and early 1930s. Radio researchers Leo C. Young and Albert Hoyt Taylor formulated the idea of using "pulses of energy for target detection" after incidents in which their radio transmissions were blocked by passing ships and aircraft (Rinehart, 2004). As with other forms of remote sensing, the military value of radar was made extremely evident during World War II. All of the major military powers (USA, England, Germany, Russia, Japan, Italy) actively worked on the design and utilization of radar systems, which advanced the technology and lead to further development in the post-war years (Rinehart, 2004). These early systems relied on a fixed-point antenna, the physical area of which determined linear resolution. With a traditional real aperture system, beam-width increases with range, inherently causing angular resolution to decrease and minimum resolvable distance to increase. Small objects could not be distinguished as range increased.

The solution to the problem of angular resolution decreasing in proportion to range came in the form of the Side Looking Airborne Radar (SLAR) systems in the 1950s. SLAR sensor systems were mounted on moving airborne platforms in which the forward advancement of

the sensor essentially "produced the equivalent effect of an extremely long antenna which expands in length in direct proportion to radar range… providing a linear resolution in the azimuth direction that is constant for all radar ranges" (Cutrona, et al., 1961). SLAR systems utilized real-aperture systems, but soon lead to the development of SAR systems. The data received in both SLAR and SAR systems are stored as the platform (airplane or satellite) advances and is then processed to produce a synthesized image of the received backscatter. While the early uses of this technology were military-driven and were therefore classified, the National Aeronautics and Space Administration (NASA) began developing SAR for civilian use beginning in the late 1960s (Franceschetti and Lanari, 1999).

Some of the earliest recognized advantages of SAR over photographic sensors for ground studies were that radar imaging missions were limited by neither time of day nor atmospheric conditions. SAR is an active system of remote sensing, meaning that the sensor emits its own energy and collects the returned energy, giving it the ability to operate independently of solar illumination (Chan, 2008). In contrast, photographic systems are passive, meaning that they collect reflected solar energy. Furthermore, radar has the ability to penetrate cloud cover (Bamler, 2000). Tropical regions that were previously impossible to image due to constant cloud cover became possible to map for the first time (Curlander and McDonough, 1991).

3.1.1 Radar in Forest Measurement Applications

Vegetation and forest mapping applications of SLAR and SAR date to the late 1970s. The ability to image perpetually cloud-covered regions led to the use of the Motorola SLAR system for mapping vegetation in Nigeria, which constituted one of the earliest studies of radar use in vegetation mapping. Vegetation was classified in 25 categories at a 30 meter resolution (Parry, 1979). Another early vegetation study involved the use of the SEASAT synthetic aperture radar to characterize vegetation types in Virginia and Maryland at 25 meter resolution. Despite being primarily designed for oceanographic research, the interpretation of the SEASAT data displayed distinct backscatter signatures for upland and lowland vegetation types that allowed their classification (Segal 1983). While these early studies highlighted the ability of radar to distinguish vegetation from other landforms and further classify the returns into vegetation categories, the use of radar to characterize forest metrics such as density and biomass was not yet thoroughly explored.

Wu and Sader's 1987 study provided one of the earliest instances of SAR being recognized for its ability to quantify vegetation characteristics. In this study, a NASA Jet Propulsion Laboratory (JPL) fully polarimetric L-band SAR system (AIRSAR), the predecessor to UAVSAR, was flown in the Gulf Coastal Plain region, an area composed mainly of natural pine, bottomland hardwood, and swamp forest with deciduous understory present at most of the plots. Researchers were interested in establishing correlations between tree height, basal area, and biomass sampled in the field and the backscatter responses of single polarizations

and polarization ratios. Using simple linear regression, they found the highest correlation to be in the VH channel with correlation coefficient (r) values of "0.499, 0.820, and 0.682 in estimating height, basal area, and total biomass, respectively." They attributed the superiority of the VH channel over the VV and HH channels at estimating the three values due to canopy scattering being dominant in VH. This early study demonstrated the possibility for SAR to be used in forest measurement applications.

In a study closely related to our research, both in species and geographic location, Kasischke et al. (1995) examined the relationship between SAR backscatter and total above-ground biomass in 61 loblolly pine stands aged 1 to >100 years within the Duke Forest near Durham, North Carolina. The mission was flown using the AIRSAR system. They found simple linear correlation coefficient (r) values as high 0.95 for the relationship between L-band VH and total branch biomass in stands with biomass between 2 and 39 kg/m^2. The results of their study suggest the possibility of accurately modeling loblolly pine in North Carolina, however the age range of stands in this study and their position in the piedmont of NC rather than the coastal plain may result in different outcomes.

Another study described in Stellingwerf and Hussin (1997) found high correlations between L-band backscatter and forest parameters in young (4-17 years) slash pine stands, but low correlations with older, more developed stands (15-20 and 16-53 years). They attributed the success of estimating the parameters of the young stands to the more drastic changes to the canopy cover in the 4-17 year old stands. These studies, as well as a number of others

(Dobson, et al., 1992; Imhoff, 1995) have shown that backscatter from the HV channel characterizes basal area and biomass more accurately than either the HH or VV channels. At least one study (Wu, 1987), however, found the strongest correlation in the VV channel when estimating total biomass of plantation stands of slash pine in the Gulf Coast Plain, again using the JPL AIRSAR L-band system. The L-band wavelength (~20cm) has been shown to better characterize woody stem structure than shorter wavelength radar (C-band, X-band), which are better suited for characterizing the vegetation in the canopy. The relationship between size of the scattering mechanism and wavelength is responsible for the greater canopy penetration of L-band radar (Dobson, 2000).

Previous studies display the potential usefulness of radar for estimating biophysical forest parameters. These studies were performed under varying regions, tree species, and ranges of biomass and basal area. This study intends to expand that body of research by examining the feasibility of using the UAVSAR L-band radar system to characterize basal area and total biomass in loblolly pine stands found in the North Carolina coastal plain.

3.1.2 Polarimetric SAR

The polarization of radar energy refers to the orientation of the electric field that is transmitted and received (Figure 1). HH-channel SAR data refers to energy that has been transmitted so that the electric field vibrates along the horizontal axis. Reflected energy that returns to the sensor in the horizontal orientation is collected and recorded. Conversely, VV-

channel SAR is the vertically-polarized energy collected by the sensor that has been transmitted in vertical orientation. Most surfaces will reflect energy in the same polarization that was transmitted. However, vegetation often de-polarizes radar energy, meaning that horizontally polarized energy that strikes leaves and branches in the canopy may be reflected in vertical orientation, or vice versa. This phenomenon means that if data is transmitted in one orientation but the sensor only collects data that is returned in the opposite orientation, vegetation will be displayed much brighter than surfaces such as water and bare soil that do not have this unique de-polarizing property (Short, 2010). Our study will examine how each of these channels (HH, VV, and HV) respond to loblolly pine stands.

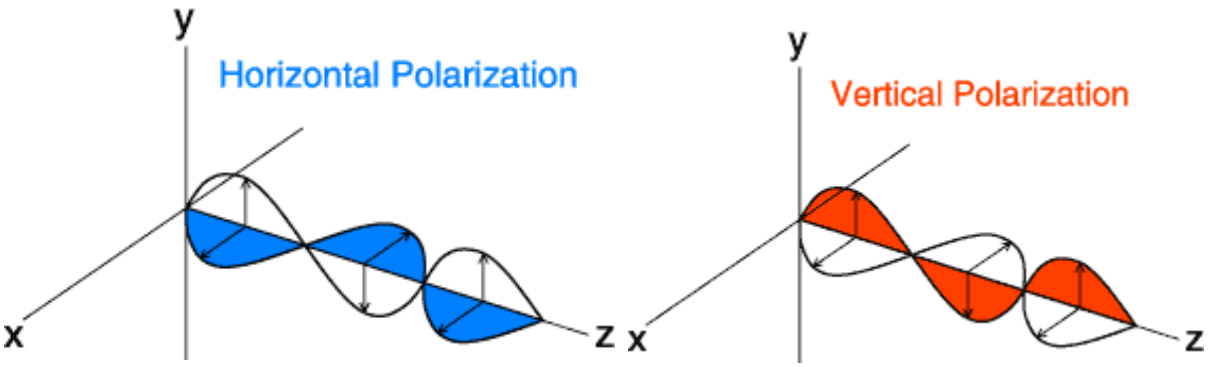

Figure 1. Polarization of radar energy. The electric field is displayed in blue for the horizontal polarization and orange for the vertical polarization (Schuur, 2003).

4. Study Area

This project focuses on a rectangular swath of the Neuse River Basin approximately 180 kilometers long by 21 kilometers wide in which UAVSAR data were collected in August 2009. The 3780 km^2 swath runs approximately from Wilson, NC in the northwest to Cape Lookout and the Southcore Banks in the southeast (Figure 2). The entire study site is within the North Carolina coastal plain region. The coastal plain region comprises approximately 45% of the land area in North Carolina. The region is characterized by low-lying, relatively flat terrain with sandy soils. The majority of North Carolina's wetland areas are present within the region (Orr and Stuart, 2000).

Figure 2. UAVSAR L-band multi-polarized radar swath used in this study. Background image courtesy of ©2011 Google.

5. Data

The following sections describe the different types of data used within this study and the software used to process these data.

5.1 UAVSAR

UAVSAR, launched by NASA JPL, is a fully polarimetric L-band radar system mounted in a pod on a Gulfstream III jet. The UAVSAR dataset, flown August 13, 2009, was acquired by the Landscape Characterization Branch of the USEPA from the NASA JPL. This UAVSAR dataset is multi-looked polarimetric (HH, VV, HV) GRD format data orthorectified with an equiangular geographic coordinate system (longitude and latitude). The fourth channel, VH, was excluded due to the "reciprocity principle of electromagnetic wave scattering," meaning that "HV and VH polarization data contains identical radar signatures" (Wu and Sader, 1987). The GRD data have been sampled to 6m x 6m pixel size. Within each pixel, there are 12 looks in the azimuth and 3 looks in the range, for a total of 36 looks per pixel. This implies that the sensor measured the returns from 36 "looks" at each pixel during a single sweep and calculated the average in order to reduce speckle noise in the final product (Franceschetti and Lanari, 1999). Linear power units (watts) are used in place of decibel units to measure returned backscatter intensity (NASA JPL, 2011). The dataset was pre-processed by the Landscape Characterization Branch to convert the files to .img format for compatibility with ERDAS Imagine software.

5.2 Field Survey Data

In order to accurately characterize the relationship between UAVSAR data and loblolly pine stand basal area and biomass, collecting *in situ* measurements was necessary. The field measurements took place during 4 weekends in late January and early February of 2011. In total, 24 sample sites were used in the final analysis. The 18 month period between radar data collection and field measurements is not ideal due to the introduction of variability in growth between stands. However, with only one complete growing cycle between the collection dates, the impact of the growth is expected to be minimal. At a mean height of 24.6 meters, we are measuring predominately semi-mature to mature loblolly pine stands that have slowed in their growth (Figure 3). While we would have preferred to have collected both radar data and field measurements on the same day, a time difference is often unavoidable in remote sensing studies.

A georeferenced ESRI shapefile of the sample loblolly pine stand sites was created. It contained the following fields: Site ID, X coordinate, Y coordinate, Basal Area (square meters/hectare), Biomass (Tons/Hectare), Average Canopy Height, Forest Type, and Notes. The shapefile was left in geographic coordinate system format.

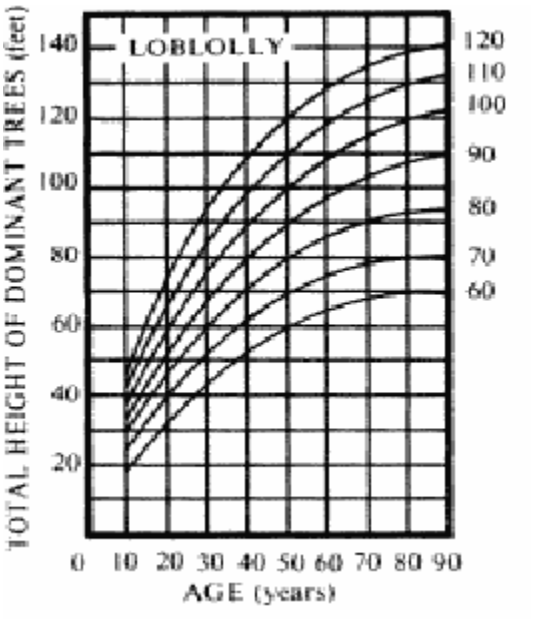

Figure 3. Growth curves based on site index of loblolly pine aged 0 – 90 years (Gunter, 1987).

5.3 Bing Maps Aerial Imagery

Microsoft Bing provides seamless aerial imagery that can be accessed through ESRI ArcMap. The high-resolution Bing imagery was used as a base layer in ArcMap and the shapefile of sample site points was overlayed. The imagery was used to verify that the points fell in the correct locations.

5.4 Software

The following is a list of software utilized at various stages throughout the project and the capacity in which they were used:

ERDAS Imagine 9.3 –Visualization and model building for backscatter intensity extraction.
ESRI ArcGIS 9.3 – Visualization, creation of shapefiles, and exportation of shapefile data.
Google Earth – Visualization of study area and field survey trip planning.
Microsoft Bing Aerial Imagery extension for ArcMap – Accuracy verification of shapefile location.
Microsoft Excel – Organization of data, statistical analysis.

6. Methods

The following sections provide a description of the steps taken to collect field measurements at sample sites, model biomass, and develop a model to determine the radar backscatter values at each site.

6.1 Field Survey Sample Sites

During late January and early February 2011, sample measurements were collected at loblolly pine forests throughout the Neuse River Basin.

6.1.1 Sample Site Selection

Initially a stratified random sampling scheme was chosen to select the locations for field measurements. The boundaries of the radar swath provided the outer limit and this broken into smaller 10.5 x10.5 km square sections. Evergreen forests were isolated for sampling by using the National Land Cover Database GIS coverage. Hawth's Tools, an application for use with ArcMap, was used to generate random points within each section. However, it was quickly discovered that using this technique would make field work impractical due to issues with physical access to sites as well as legal access given that much of the land is privately held. Due to these limitations, a more subjective, but far simpler approach was taken.

During the planning stages of each field trip, Google Earth overlayed with a KML file of the swath boundaries was utilized to search for sample sites. Potential locations were identified and recorded in order to make the field trips more time efficient. These sample locations were selected based on a number of qualitative criteria. Potential loblolly pine dominated areas were selected by viewing winter imagery so that leaf-off hardwood stands could be excluded. The stands had to be reasonably accessible from a road way. The sites were also required to be relatively homogenous so that the sample basal area measurements would be representative of a relatively large area. This was to allow for any minor errors in GPS coordinates or in the georectificaiton of the UAVSAR data. For the same reason, the center point of each sample site had to be at least 50-meters away from other land cover types, such as roads or agricultural fields. This ensured that non-forest land cover would not be included

in the sampled UAVSAR data. Finally, we sought to distribute the sample sites throughout as much of the swath as possible. The south-eastern portion of the swath was not represented in the sampling scheme, due to time and financial limitations. In total, 24 of the loblolly pine stands visited were included in the final sample set.

6.1.2 Sample Site Field Measurements

At each sample site, a number of measurements were recorded. Upon selecting a relatively homogenous area of forest, a center point for each survey was selected and marked using a stake. A Garmin GPSMAP 62S GPS receiver was used to record the location of the center point. Notes were recorded about each site, such as dominant species, understory conditions, etc. For reference, 10 digital photographs were taken at each location. 1 photograph was taken vertically and 8 were taken at an oblique angle at N, NE, E, SE, S, SW, W, and NW orientations in order to characterize the trunk and canopy density. One photograph was taken horizontal to the ground to characterize the understory.

The mean canopy height of each stand was measured by selecting three trees based on their representation of the average canopy height. Though somewhat subjective, the time and financial constraints of the field work had to be considered again. The height of each tree was then calculated by moving to the farthest position at which the top of the crown was visibleand using a clinometers to take an angular measurement (percent slope) from the base

of the trunk to the top of the crown. The height was then established using the following formula:

$$[(\text{PS}) \times (\text{DM})] / 100 = \text{Tree Height} \quad [1]$$

where PS indicates percent slope measured by the clinometer and DM indicates distance from the center of the tree to the measurement site. The average canopy height for the stand was then estimated by calculating the mean of the three tree heights.

Basal area measurements at the sample sites were determined using a wedge prism. The basal area prism is a sampling device that allowed us to make relatively quick estimates of the basal area of the forested stand. The prism used in this study was designed to provide square feet of trunk per acre based on the number of trees meeting "in" criteria multiplied by a basal area factor (BAF) of 10. The number of "in" trees were recorded throughout this process along with their respective diameters at breast height (DBH).

In this study, trees that were borderline were not counted "in" or "out" alternately, as is sometimes practiced. To provide a more accurate sample, the distance from the site center point to the center of the borderline tree was measured along with the DBH. The trees were then determined to be "in" or "out" based on a limiting distance for a given DBH. The equation for calculating the limiting distance of the plot radius is as follows:

$$LD = 0.33d \quad [2]$$

where *d* is DBH in centimeters and LD is the maximum distance from the plot center that a tree of a given *d* can be counted as "in." For example, if a borderline tree was measured at a distance of 10.0 meters from the site center, it would need to have a DBH value of at least 30.3cm to be "in."

After returning from each field trip, data collected at each site were entered in spreadsheets using Microsoft Excel.

6.1.3 Total Biomass Measurements

The decision to correlate biomass and UAVSAR backscatter came after the field survey. Height measurements, which are a necessary input when modeling biomass, were not made in conjunction with the DBH measurements of individual trees because that was not a necessary function of the initial objective to determine basal area. Given the limitation of the sample data available to us, it was necessary to model the heights of the loblolly pines based on the known DBH values. Once height was estimated for the trees within the sample plots, it was possible to model total biomass of the individual trees and extrapolate the calculations to the hectare level.

Trincado's 2006 study provides an approach for calculating the heights of individual loblolly pine trees in the Coastal Plain region using DBH as the only input. Trincado found that

loblolly pine heights could be more accurately calculated using a calibrated model in the study by inputting the height-diameter relationships of the three trees from each stand. Our study had to be limited to the DBH-only model using this equation:

$$h = 1.37 + 4.0779\, d^{0.4386} \quad [3]$$

where h is tree height in meters and d is DBH in centimeters.

With the heights and diameters of the trees in the sample stands established, total biomass for individual loblolly pine trees was modeled using the equation presented in Williams' (2006) study. This regression model was found to have an r^2 value of 0.934

:

$$\text{Total Biomass (kg)} = 0.0201 d^2 h + 14.995 \quad [4]$$

Once the total biomass of the individual sampled trees was estimated, the results were extrapolated to the hectare level. For each tree sampled, a trees per hectare (TPH) value was calculated. The TPH represented the approximate number of trees of that particular diameter assumed to be in a one hectare value. TPH is calculated based on the plot radius limiting distance of a sampled tree of a given diameter. For example, a tree with a DBH of 25cm has a plot radius of 8.25m (25cm x 0.33) which equates to a 213.72 m^2 plot. It can then be "tacitly assumed" that 46.79 trees of this DBH will be found in 1 hectare of the surveyed forest (presuming a relatively homogenous forest type) (Avery and Burkhart, 1994).

The total biomass for each sample tree was then multiplied by their respective TPH value. The sum of the total biomass values represents the total biomass of all the trees within the one hectare sample location. This final value was used as the input variable for each site when calculating correlation with UAVSAR backscatter. A summary of biomass and basal area values for each of the sites is shown in Table 1 and summary statistics for the combined stands, plantation only, and natural only are show in Tables 2, 3 and 4, respectively.

Table 1. Summary of the type (N=natural stand; P=plantation), basal area, and biomass of the 24 sample sites.

Site Number	Type	BA m^2/Ha	Biomass T/Ha
1	N	29.84201	65.93
2	N	36.72863	120.02
3	N	41.3197	161.36
5	P	20.65985	89.54
6	P	20.65985	106.6
7	P	18.36431	95.02
10	P	50.50186	248.12
11	P	52.7974	262.27
12	P	50.50186	246.54
13	N	45.91078	197.06
14	N	45.91078	177.25
15	N	48.20632	187.02
16	N	34.43309	165.39
17	N	34.43309	164.6
18	P	16.06877	80.44
19	P	16.06877	81.66
20	P	18.36431	93.48
23	N	32.13755	101.75
24	P	25.25093	127.3
27	N	36.72863	169.48
29	N	16.06877	87.21
35	P	16.06877	112.73
36	P	11.4777	79.33
37	P	16.06877	98.83

Table 2. Summary statistics of all 24 sample sites.

	BA M^2/Ha	Biomass M^2/ha
Min	11.48	65.93
Max	52.80	262.27
Range	41.32	196.34
Median	30.99	116.38
Mean	30.61	138.29
Std Dev	13.28	57.22

Table 3. Summary statistics of the 13 plantation stands.

	BA M^2/Ha	Biomass M^2/Ha
Min	11.48	79.33
Max	52.80	262.27
Range	41.32	182.94
Median	18.36	98.83
Mean	25.60	132.45
Std Dev	14.40	66.98

Table 4. Summary statistics of the 11 natural loblolly pine stands.

	BA M^2/Ha	Biomass M^2/Ha
Min	16.07	65.93
Max	48.21	197.06
Range	32.14	131.13
Median	36.73	164.60
Mean	36.52	145.19
Std Dev	8.67	41.85

6.2 Creating Point Shapefile

All of the data collected during the field surveys was entered in Excel spreadsheets in a format that was compatible with creating ESRI ArcMap shapefiles. The spreadsheet contained X,Y latitude/longitude coordinates collected with GPS at each site along with descriptive attributes. The Excel spreadsheets were then imported into ArcMap using the "Add XY Data" tool and converted to a shapefile using the "Export" tool. The final shapefile contains the following fields: Site ID, X coordinate, Y coordinate, Basal Area (square meters/hectare), Biomass (Tons/Hectare), Average Canopy Height, Forest Type, and Notes.

The resulting shapefile was overlayed onto a boundary polygon of the UAVSAR swath and Bing Maps Aerial Imagery in order to visually check for accuracy of the GPS coordinates (Figure 4). While minor location-based inaccuracies within the relatively homogenous landscape of the sample sites could not be detected by eye, major errors could be easily spotted. Two sites were discarded due to inadvertently straying outside of the UAVSAR data swath boundaries while performing field work, resulting in a final sample size of 24 sites.

Figure 4. Shapefile of sample sites overlayed on Bing Aerial Imagery and boundary of UAVSAR swath.

6.3 UAVSAR Data Processing

With a point shapefile of the sample sites created, the next step was to relate the sample points to the corresponding UAVSAR backscatter intensity values. Intensity values were extracted from three sizes of pixel windows that were created around each point (Figure

5).These three window sizes (3x3, 5x5, and 7x7) represented approximately 324 m^2, 900 m^2, and 1764 m^2 on the ground, respectively. For each window, we wanted to determine the mean, minimum, and maximum values of the pixels within.

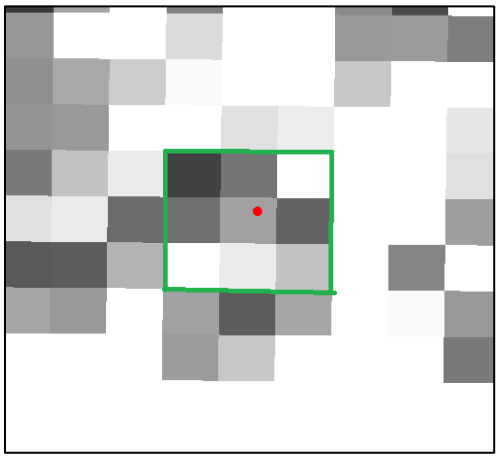

Figure 5. Illustration of a 3x3 pixel window (in green) overlayed on the UAVSAR image. The sample site point is shown in red.

To begin processing, it was necessary to prepare the UAVSAR data and create models in ERDAS Imagine. Given the large size of the dataset (~8 GB), which would make processing impractical, it was necessary to reduce the size of the image. To reduce processing time we eliminated areas that did not contain sample sites.

Next, a model was designed in the ERDAS Imagine Model Maker to extract the UAVSAR backscatter values. The model was designed to input the point shapefile, the UAVSAR image, and a matrix that determines the size of the window. A Focal Mean, Min, or Max

expression was used to extract values for each window size. The output was a raster file that replaced the value of each pixel in the UAVSAR dataset with the mean, min, or max value for the specified window size around each pixel (Figure 6).

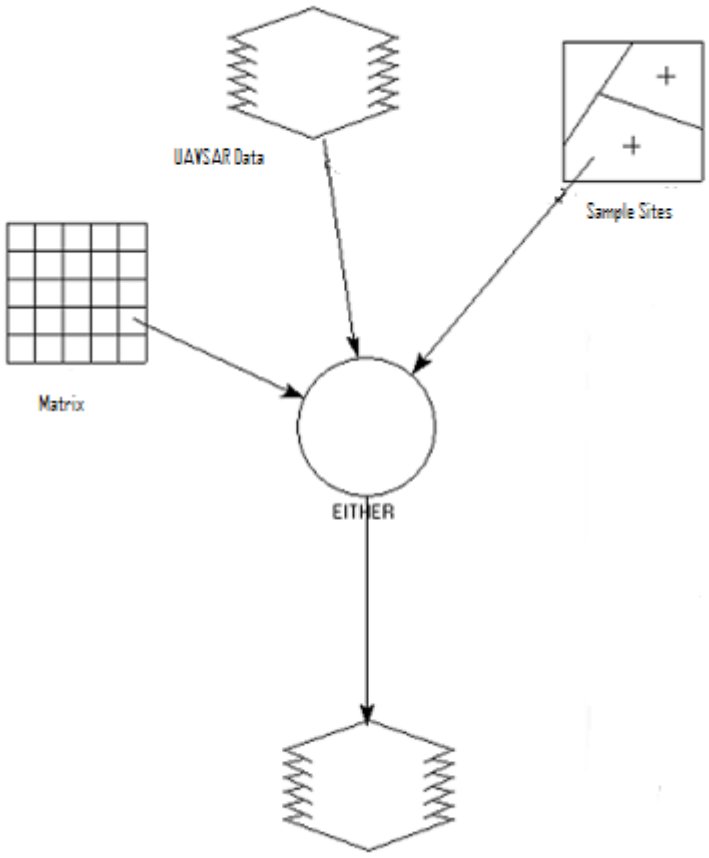

Figure 6. ERDAS Imagine model for extracting UAVSAR backscatter values.

The next task was to combine the sample site points with their associated mean, max, or min backscatter intensity values from the outputted raster images. To do so, the “Extract Values

to Points" tool in ArcMap was used. That tool extracted the cell values of the raster and added them as a field to each of the overlying points in the sample sites shapefile.

6.4 Analysis of Results

Once each of the sample sites had backscatter intensity values associated with them in their respective shapefiles, analysis of the correlations began. To plot basal area and biomass against backscatter intensity and calculate R^2 values, data from the shapefiles needed to be brought into spreadsheet format in Excel. To do so, the attributes of the shapefiles were exported as .dbf files. Once exported to Excel, scatter plots of biomass basal area against backscatter intensity and associated R^2 values were calculated.

7. Results and Discussion

162 scatter plots and associated R^2 values were generated to display the relationship between UAVSAR backscatter intensity and loblolly pine-dominated forest basal area and total biomass for the three sample groups (All Stands, Natural Stands, and Plantation). Each combination of the 27 combinations of window size (3x3, 5x5, 7x7), statistical operation (min, max, mean), and polarization (HH, HV, VV) was examined for basal area and biomass for each of the three sample groups (2 x 3 x 27 = 162 analyses).

7.1 Correlation Between UAVSAR Backscatter Intensity and Basal Area

All 82 combinations (27 per sample group) of polarization, pixel window size, and statistical operation had relatively low R^2 values when the *in situ* measurements of basal area were analyzed against the UAVSAR backscatter intensity data. In each of the three groups the highest correlation was found with HV polarization using the minimum value in the pixel window, which is consistent with similar studies. The highest R^2 values were 0.2107, 0.5251, and 0.3435 in the All Stands, Plantation, and Natural groups, respectively. The 5x5 pixel windows had higher correlation for All Stands and Plantation Stands, while Natural Stands had best results using a 3x3 pixel window. HH band showed the lowest sensitivity to basal area, which had been anticipated. Matrices of the R^2 values are displayed in Tables 5, 6, and 7.

Table 5. R2 values for each of the 27 combinations of pixel window size, polarization, and statistical operation when comparing basal area to UAVSAR backscatter in all 24 loblolly pine stands.

All Stands Correlation of Backscatter Intensity with Basal Area				
		R^2 Values		
Window Size	**Polarization**	**Min**	**Max**	**Mean**
3x3	HH	0.0109	0.0673	0.00003
3x3	VV	0.1078	0.042	0.0014
3x3	HV	0.0398	0.067	0.0048
5x5	HH	0.0002	0.0726	0.0011
5x5	VV	0.0585	0.0134	0.0247
5x5	HV	**0.2107**	8.00E-06	0.0506
7x7	HH	0.0108	0.0628	0.0022
7x7	VV	0.0133	0.0003	0.0185
7x7	HV	0.1646	0.0189	0.0185

Table 6. R2 values for each of the 27 combinations of pixel window size, polarization, and statistical operation when comparing basal area to UAVSAR backscatter in the 13 plantation loblolly pine stands.

Plantation Stands Correlation of Backscatter Intensity with Basal Area				
		R^2 Values		
Window Size	**Polarization**	**Min**	**Max**	**Mean**
3x3	HH	0.1073	0.0511	0.0277
3x3	VV	0.2683	0.0513	8.00E-05
3x3	HV	0.0668	0.0636	0.0006
5x5	HH	0.1079	0.0977	0.0517
5x5	VV	0.2083	0.0275	0.0072
5x5	HV	**0.5251**	2.00E-04	0.1175
7x7	HH	0.1702	0.2172	0.0604
7x7	VV	0.1906	0.0126	0.0071
7x7	HV	0.4424	0.0219	0.1992

Table 7. R2 values for each of the 27 combinations of pixel window size, polarization, and statistical operation when comparing basal area to UAVSAR backscatter in the 11 natural loblolly pine stands.

Natural Stands Correlation of Backscatter Intensity with Basal Area				
		R^2 Values		
Window Size	**Polarization**	**Min**	**Max**	**Mean**
3x3	HH	0.0004	0.1009	0.044
3x3	VV	0.2008	0.0034	0.0784
3x3	HV	**0.3435**	0.111	0.1779
5x5	HH	0.0023	0.0171	0.1341
5x5	VV	0.2324	0.0501	0.227
5x5	HV	0.2374	0.2605	0.2923
7x7	HH	1.00E-04	0.0642	0.037
7x7	VV	0.043	0.0665	0.1038
7x7	HV	0.0904	0.1438	0.168

7.2 Correlation Between UAVSAR Backscatter Intensity and Total Biomass

Much like the analyses of basal area, all 82 combinations of polarization, pixel window size, and statistical operation showed low R^2 values when the modeled calculations of total biomass of the 3 groups of sample sites were analyzed against the UAVSAR backscatter intensity data. As was the case with basal area, the highest correlations were again found in the HV band in all three groups. All three groups had the highest correlation in the 5x5 window size, with the All Stands and Plantation groups having best results using the

minimum values. The Natural group, on the other hand had the best results using the mean value of the window, which resulted in the highest correlation of the entire study at an R^2 value of 0.6107. The All Stands and Plantation Stands groups had maximum R^2 values of 0.334 and 0.4885, respectively. Matrices of the R^2 values are displayed in Tables 8, 9, and 10.

Table 8. R^2 values for each of the 27 combinations of pixel window size, polarization, and statistical operation when comparing total biomass to UAVSAR backscatter in all loblolly pine stands.

All Stands **Correlation of Backscatter Intensity with Total Biomass** **R^2 Values**				
Window Size	**Polarization**	**Min**	**Max**	**Mean**
3x3	HH	0.072	0.0384	0.0077
3x3	VV	0.1931	0.0377	0.0127
3x3	HV	0.1253	0.0082	0.0615
5x5	HH	0.0392	0.0682	0.0086
5x5	VV	0.1679	0.0381	0.0791
5x5	HV	**0.334**	0.0488	0.2003
7x7	HH	0.0642	0.1516	0.0002
7x7	VV	0.0925	0.0001	0.0432
7x7	HV	0.2893	0.0573	0.2049

Table 9. R^2 values for each of the 27 combinations of pixel window size, polarization, and statistical operation when comparing total biomass to UAVSAR backscatter in natural loblolly pine stands.

Natural Stands **Correlation of Backscatter Intensity with Total Biomass**				
		R^2 Values		
Window Size	**Polarization**	**Min**	**Max**	**Mean**
3x3	HH	0.1065	0.0134	0.2227
3x3	VV	0.3358	0.0002	0.1384
3x3	HV	0.3759	0.1536	0.3836
5x5	HH	0.0336	0.0244	0.2613
5x5	VV	0.5108	0.1116	0.3951
5x5	HV	0.3407	0.4189	**0.6107**
7x7	HH	0.0569	0.2167	0.0352
7x7	VV	0.1883	0.0273	0.1358
7x7	HV	0.2742	0.1984	0.3974

Table 10. R^2 values for each of the 27 combinations of pixel window size, polarization, and statistical operation when comparing total biomass to UAVSAR backscatter in plantation loblolly pine stands.

Plantation Stands Correlation of Backscatter Intensity with Total Biomass				
		R^2 Values		
Window Size	**Polarization**	**Min**	**Max**	**Mean**
3x3	HH	0.0971	0.0607	0.0245
3x3	VV	0.2056	0.0772	0.0004
3x3	HV	0.1097	0.0452	0.0038
5x5	HH	0.1009	0.0949	0.0265
5x5	VV	0.1282	0.024	0.0055
5x5	HV	**0.4885**	0.0068	0.1348
7x7	HH	0.1361	0.1839	0.0308
7x7	VV	0.1457	0.0035	0.0166
7x7	HV	0.3805	0.0328	0.2125

7.4 Discussion of Results

There are a number of factors that may have introduced error into this study and contributed to the low correlation between UAVSAR data and the forest density measurements.

As discussed earlier, the time difference between radar collection and field data collection may have impacted the results. While it is unlikely that growth and other within stand changes (tree/limb loss due to storms, insects, disease, etc.) during this 18-month period

caused a major reduction in correlation, it is quite possible that some accuracy was lost in the study. During this period, the growth rates between individual loblolly pine stands may have been influenced by factors such as soil quality, stand age and density. It would be very difficult to determine the effect of these factors and apply them to this study. However, this is a problem inherent to many remote sensing studies as it is often not possible to have imagery acquired at the same time as the field measurements.

Another factor that may have introduced error is the inclusion of both natural pine stands and plantation pine stands in the All Stands sample population. Focusing on a single type of stand in each analysis displayed greater sensitivity. While the initial objective of the study was to determine the feasibility of modeling loblolly pine forests as a whole, the varying conditions encountered in a natural stands versus plantation stands decrease the sensitivity of radar backscatter to biomass and basal area, which has been shown in previous research (Kasischke, 1995).

It is likely that the modeled values of total biomass at the sample sites contained a substantial amount of error. A more accurate model of biomass could have been calculated if the model from Trincado's 2006 study had been calibrated using a sample of individual tree height/DBH relationships. As mentioned earlier in the text, however, the initial focus of the study did not include biomass, so the field trips did not include the ideal measurements for calculating biomass. Though canopy height was measured by calculating the mean of three representative trees at each site, the heights were not recorded in relation to the DBH values

of the respective trees. As such, the simplified method of modeling biomass that was used in this study was the only option without re-visiting each of the sample sites. Time and funding constraints prevented that option.

Another contributor to weak correlations may have been caused by position error of the sample sites in relation to the backscatter data due to image registration or GPS inaccuracies. The Garmin GPS unit, with Wide Area Augmentation System (WAAS) enabled, may have had error up to 5m. There may also be slight inaccuracies in NASA JPL's image registration process that could lead to further positional discrepancies. However, the use of different window sizes was designed to reduce these effects. The selection of sites that were relatively homogenous within a minimum of a 50m x 50m area was also done to account for positional error.

The backscatter data may have shown higher correlations if a moving window filtering process had been used to reduce speckle-noise (Wu and Sader, 1987). The sensitivity of radar has been shown to decrease due to speckle noise in areas less than 1.0 ha (Saatchi, et. al, 2011). Visual inspection of the backscatter data displays substantial variation in reflection intensity in relatively homogenous (Figure 7). Table 11 provides a summary of the HV backscatter intensity mean, range, standard deviation, and coefficient of variation values found in the 3 x 3 pixel window size. Coefficient of variation is a simple ratio of standard deviation divided by mean. It provides a normalized measure of variation that can be used for comparison between the different sites. As can be seen in the example in Table 11, the coefficient of variation exceeds the mean at many of the sites. This suggests that the signal-

to-noise ratio may be too low for the data to be useful in its current state. Further processing using filters to smooth noise in the data may be necessary.

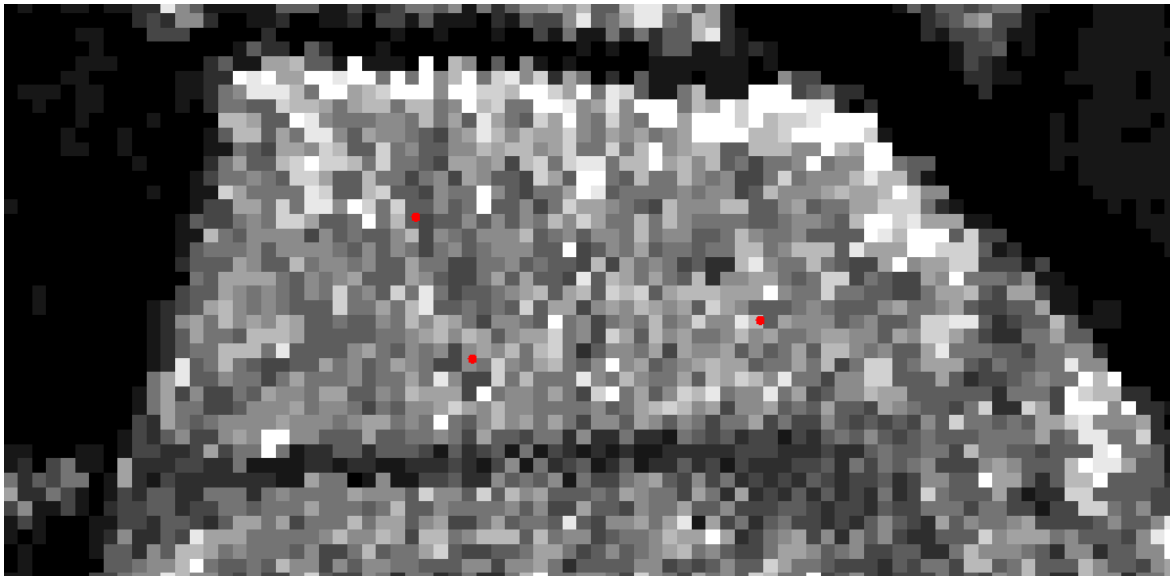

Figure 7. Speckle noise present in homogenous forests. This particular plot is a Loblolly Pine plantation outside of Wilson, NC.

Table 11. Within-stand HV backscatter intensity variability for a 3 x 3 pixel (18m x 18m) window surrounding each sample site center point.

Within Stand Variation - 3x3 HV					
Site	**Type**	**Mean**	**Range**	**Std Dev**	**C of V**
1	N	0.122771	0.203092	0.055034	0.448263
2	N	0.286514	0.413706	0.121566	0.424292
3	N	0.283513	0.398182	0.120399	0.424669
13	N	0.347552	0.145386	0.042701	0.122861
14	N	0.491514	0.373297	0.107654	0.219024
15	N	0.458841	0.434111	0.13426	0.292607
16	N	0.342215	0.334832	0.10593	0.309542
17	N	0.342965	0.277429	0.090348	0.263431
23	N	0.399057	0.430324	0.166059	0.416129
27	N	0.397023	0.470261	0.156959	0.39534
29	N	0.341104	0.398024	0.157304	0.461163
5	P	0.317444	0.550858	0.156559	0.493185
6	P	0.305821	0.35669	0.108853	0.355938
7	P	0.286359	0.199934	0.074818	0.261275
10	P	0.395114	0.403456	0.146756	0.371427
11	P	0.333292	0.291247	0.114181	0.342584
12	P	0.446053	0.458348	0.147174	0.329947
18	P	0.497222	0.569221	0.190374	0.382876
19	P	0.388297	0.631355	0.176309	0.454058
20	P	0.389171	0.380017	0.146984	0.377686
24	P	0.419206	0.601098	0.187888	0.448201
35	P	0.463592	0.686389	0.19635	0.423541
36	P	0.407511	0.722833	0.216604	0.53153
37	P	0.311962	0.265754	0.097943	0.313958

The most substantial contributor to the weak correlations was likely the saturation of backscatter at a forest density threshold below the majority of the sample sites. A number of studies have shown that backscatter saturates, becoming unresponsive to increases in biomass

or basal area beyond a certain threshold (Dobson, et al., 1992; Kasischke, et. al., 1995). While many studies have displayed linear responses of L-band backscatter to biomass at certain levels, backscatter has been shown to be unresponsive once biomass approaches 60-100 tons/Ha in loblolly pine (Dobson, et al., 1992; Rauste, et al., 1994). Imhoff (1993; 1995) and Wang et al. (2006) determined that L-band backscatter was largely saturated at only 40 tons/Ha and another study placed L-band saturation at approximately 60-80 tons/Ha (Lucas, 2000).

L-band radar, while more accurate for estimating biomass than C-band or X-band radar, reaches saturation at lower biomass levels than P-band (Kasischke, et al., 1995). The overall usefulness for L-band radar for characterizing developed forests may be limited to regenerating stands (Dobson, 2000). As the canopies of loblolly pine stands surpass a certain density and biomass level, L-band energy is "largely attenuated by branches and needles" (Kasischke, et al., 1995) rather than characterizing the large stems of individual trees which is necessary for estimating basal area and biomass (Hussin, et al., 1991). Figure 8 provides a diagram of how radar energy reflects in trees. Double-bounce reflectance, in which the energy is not attenuated by the canopy, is the result of being reflected from the ground to the main stems (or vice versa) and returning to the sensor. This would likely be the ideal type of reflectance for characterizing basal area. Volumetric scattering, however, may be the dominant type of reflectance once saturation has been reached due to dense canopy.

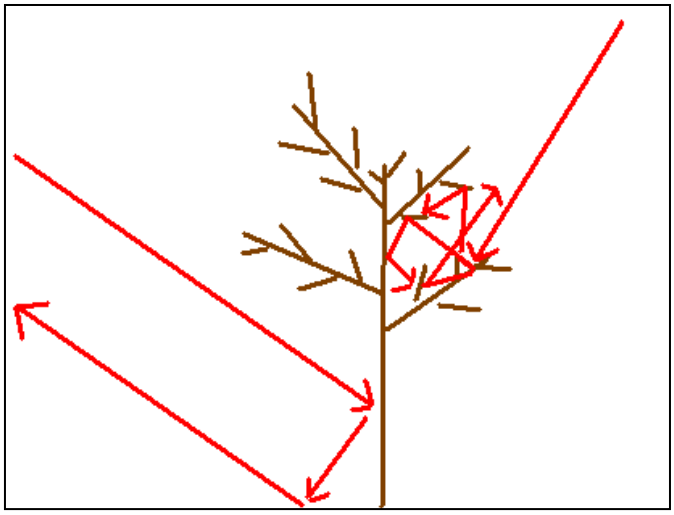

Figure 8. Diagram of radar reflectance of a tree. Double-bounce is shown on left. Volumetric scattering shown on right.

Furthermore, it is likely that understory plays a role in the interaction between backscatter and forest stem structure. The existing literature does not draw definitive conclusions about this relationship, but we think it is likely that the deciduous understory found in our sample sites resulted in lower correlations than if no understory was present. Understory at our sample sites ranged from none at all to very dense, being difficult to hike through even in the leaf-off conditions we sampled in.

Previous studies that examined relatively young stands with open canopies and low biomass in comparison to older, denser stands have confirmed that L-band is more responsive under those parameters (Hussin, et al., 1991; Kasischke, et al., 1995; Stellingwerf and Hussin, 1997). As this study was not limited to a certain range of basal area and biomass parameters, this may have contributed to the lack of strong correlation. The majority of the sites sampled

in this study exceeded the 40-100 tons/Ha saturation range. The weak correlations we encountered were congruent with the findings of Foody et al. (1997). Further study under the environmental parameters encountered in this study will likely require the use of a different sensor system in the P-band wavelength. A concise table of operating sensors follows (Table 12). The European Space Agency has been actively seeking to launch a satellite-borne p-band SAR system as part of their BIOMASS mission, with the intent of complete mapping of global biomass (Scipal et al., 2010). The program has not yet reached fruition, but if it is launched the satellite will make p-band data more readily available to the scientific community.

Table 12. Table of sensor systems. Asterisk denotes that sensor is no longer operating.

Name	**Band (s)**	**Platform**	**Country**
AIRSAR*	C, L, P	Airborne	USA
E-SAR	X, C, L, P	Airborne	Germany
GeoSAR	X, P	Airborne	USA
PiSAR	L	Airborne	Japan
PalSAR	L	Satellite	Japan
SETHI	P	Airborne	France

While the correlations founds in this study were too low to proceed with modeling the biomass and basal area of loblolly stands throughout the coastal plain, future studies with higher correlations could be used to generate a surface map of biomass. The value of the map would need to be evaluated through an accuracy assessment. Validation through field measurements would be necessary at a number of random sample sites, but the cost of field work would be prohibitive of a gathering a large set of *in situ* measurements. Therefore, the use of pre-existing datasets of biomass and basal area field measurements such as the Forest Inventory and Analysis (FIA) database would be beneficial. The sample plots in the FIA database represent approximately one acre each and one plot is collected for every 6000 acres. The precise locations of plots are not generally provided to FIA customers due to privacy restrictions for private land holders and are instead given as a nearby (0.5 to 1 mile) set of coordinates. However, FIA offers higher precision data services on a case-by-case basis for customers involved in remote sensing projects, which this type of project would likely qualify (Woudenberg et. al., 2010). While the FIA data may not provide an absolutely definitive level of accuracy, they would serve as a very useful guide in determining which areas show positive correlations and which areas may need to be examined further through field measurements. Those areas could be stratified and assigned random points to be visited.

8. Conclusion

The primary objective of this study was to explore the feasibility of using L-band radar to estimate basal area and total biomass of mature loblolly pine stands. We found relatively weak correlations for both measures in all three sample groups. The All Stands group displayed the lowest correlations, with the highest R^2 values being only 0.2107 and 0.334 for basal area and biomass, respectively. The variability in the characteristics of mature plantation and natural loblolly pine stands lead to poor estimation of biophysical factors. Though the small sample size prevents statistical conclusions, the preliminary results found in this study suggest that basal area and biomass can be more accurately measured when plantation and natural loblolly stands are modeled as separate groups. Plantation stands displayed much higher correlations with the radar backscatter, with R^2 values 0.5251 and 0.4885 in basal area and biomass, respectively. The radar backscatter displayed an even greater sensitivity to biomass in the natural stands, with an R^2 of 0.6107, which is the highest correlation found in the entire study. However, the strongest correlation of basal area in the natural stand has a much lower R^2 of 0.3435. In all three groups, radar backscatter showed greater sensitivity to total biomass. In all cases, the HV band had the highest sensitivity while HH showed the least sensitivity. This is consistent with other studies (Wu and Sader, 1987; Kasischke, et al., 1995). The most significant problem in this study is that the forest stands we measured likely exceeded the basal area and biomass saturation thresholds for L-band radar. Had a greater range of sample stands that included juvenile stands been used, it is possible that the radar may have shown greater sensitivity.

While the sample size of this study may be too small to draw definitive conclusions, this research indicates that it is not feasible to estimate basal area and biomass of mature loblolly pine stands in the NC coastal plain using simple linear regression with L-band radar, particularly when natural and plantation stands are not analyzed separately. It would not be an economically sound decision to collect a larger set of field measurements and continue with this study as there is little indication that we can estimate basal area or biomass of loblolly pine in this region using these techniques. Future study would benefit from using longer wavelength P-band radar, due to the higher biomass saturation threshold. It may not be feasible to use L-band or shorter wavelength radar to measure these parameters in anything but young stands with lower basal areas and biomass found in this study. Furthermore, it is apparent that HV polarization should be focused on as it consistently displays the highest correlations with these types of forest measurements.

REFERENCES

American Rivers, 2007. *America's Most Endangered Rivers™ report* , American Rivers, Washington, District of Columbia.

Avery, T.E. and H.E. Burkhart, 1994. *Forest Measurements,* McGraw-Hill, Inc., 408 p.

Bamler, R., 2000. Principles of Synthetic Aperture Radar, *Surveys in Geophysics*, 21(2): 147-157.

Campbell, J. B., 2007. *Introduction to Remote Sensing*, Guilford Press, New York, New York, 622 p.

Chan, Y.K. and V.C. Koo, 2008. An Introduction to Synthetic Aperture Radar (SAR), *Progress in Electromagnetics Research B,* 2: 27-60.

Curlander, J.C. and R.N. McDonough, 1991. *Synthetic aperture radar: systems and signal processing*, John Wiley & Sons, Inc, 647 p.

Cutrona, L.J., W.E. Vivian, E.N. Leith, and G.O. Hall, 1961. A High Resolution Radar Combat-Surveillance System, *IRE Transactions on Military Electronics*, MIL-5(2): 127-131.

Dobson, M.C., F.T. Ulaby, T. LeToan, A. Beaudoin, E.S. Kasischke, and N. Christensen, 1992. Dependence of Radar Backscatter on Coniferous Forest Biomass, *IEEE Transactions on Geoscience and Remote Sensing,* 30(2): 412 - 415.

Dobson, M.C., 2000. Forest Information from Synthetic Aperture Radar, *Journal of Forestry,* 98(6): 41 - 43.

Foody, G.M., R.M. Green, R.M. Lucas, P.J. Curran, M. Honzak, I. Do Amaral, 1997. Observations on the Relationship Between SIR-C Radar Backscatter and the Biomass of Regenerating Tropical Forests, *International Journal of Remote Sensing,* 18(3): 687 - 974.

Franceschetti, G and R. Lanari, 1999. *Synthetic aperture radar processing*. Electronic Engineering Systems Series. CRC Press, 308 p.

Franklin, S.E., 2001. *Remote Sensing for Sustainable Forest Management,* CRC Press LLC, Boca Raton, Florida, 424 p.

Gilley, J.E., W.F. Sabatka, B. Eghball, and D.B. Marx, 2008. Nutrient Transport as Affected by Rate of Overland Flow, *Transaction of the ASABE,* 51(4): 1287 – 1293.

Gunter, J.E., 1987. Loblolly Pine Growth Curve, Illustration, Georgia Forest Landowner's Manual, Cooperative Extension Service, URL: http://warnell.forestry.uga.edu/service/library/b0950/b0950.pdf, The University of Georgia, Athens, Georgia (last date accessed: 28 October 2011).

Hussin, Y.A., R.M. Reich, R.M. Hoffer, 1991. Estimating Slash Pine Biomass Using Radar Backscatter, *IEEE Transaction on Geoscience and Remote Sensing,* 29(3): 427 - 431.

Imhoff, M.L., 1993. *The Dependence of Synthetic Aperture Radar Backscatter on Forest Structure and Biomass: Potential Application for Global Carbon Models*, Ph.D. Dissertation, Stanford University, Stanford, California, 280 p.

Imhoff, M.L., 1995. Radar Backscatter and Biomass Saturation: Ramifications for Global Biomass Inventory, *IEEE Transactions on Geoscience and Remote Sensing,* 33(2): 511 - 518.

Imhoff, M.L., S. Carson, P. Johnson, 1998. A Low-Frequency Radar Experiment for Measuring Vegetation Biomass, *IEEE Transactions on Geoscience and Remote Sensing*, 36(6): 1988-1991.

Kasischke, E.S., N.L. Christensen Jr., and L.L. Bourgeau-Chavez, 1995. Correlating Radar Backscatter with Components of Biomass in Loblolly Pine Forests, *IEEE Transactions on Geoscience and Remote Sensing*, 33(3): 643-659.

Kruzic, A.P. and E.D. Schroeder, 1990. Nitrogen Removal in the Overland Flow Wastewater Treatment Process-Removal Mechanisms, *Water Environment Federation,* 62(7): 867 – 876.

Lucas, R.M., A.K. Milne, N. Cronin, C. Witte, and R. Denham, 2000. The Potential of Synthetic Aperture Radar (SAR) for Quantifying the Biomass of Australia's Woodlands, *Rangeland Journal,* 22(1): 124 - 140.

Lunetta, R.S., R.G. Greene, J.G. Lyon, 2005. Modeling the Distribution of Diffuse Nitrogen Sources and Sinks in the Neuse River Basin of North Carolina, USA, *Journal of the American Water Resources Association,* 41(5): 1129 – 1147.

McEldowney, R.R., M. Flenniken, G.W. Frasier, M.J. Trlica, and W.C. Leininger, 2002. Sediment Movement and Filtration in a Riparian Meadow Following Cattle Use, *Journal of Range Management,*55(4): 367 – 373.

NASA JPL, 2011. Uninhabited Aerial Vehicle Synthetic Aperture Radar, URL: http://uavsar.jpl.nasa.gov/, National Aeronautics and Space Administration, - Jet Propulsion Laboratory, Pasadena, California (last date accessed: 1 November 2011).

North Carolina Forest Service (NCFS), 2010. Conserving Working Forest, North Carolina's Forest Resources Assessment: A statewide analysis of the past, current and projected future conditions of North Carolina's forest resources 2010, URL: http://www.ncforestassessment.com/PDF/NC%20Forest%20Assessment%20Complete.pdf, North Carolina Forest Service, Raleigh, North Carolina (last date accessed: 27 October 2011).

Orr, D.M. and A.W. Stuart, 2000. *The North Carolina atlas: portrait for a new century,* The University of North Carolina Press, Chapel Hill, North Carolina, 480 p.

Paerl, H.W., J.L. Pinckney, J.M. Fear, B.L. Peierls, 1998. Ecosystem Responses to Internal and Watershed Organic Matter Loading: Consequences for Hypoxia in the Eutrophying Neuse River Estuary, North Carolina, USA, *Marine Ecology Progress Series,* 166: 17-25.

Parry, D.E, 1979. Mapping Nigeria's Vegetation From Radar, *The Geographical Journal*,145: 265-274.

Rauste, Y., T. Hame, J. Pulliainen, K. Heiska, M. Hallikainen, 1994. Radar-based Forest Biomass Estimation, *International Journal of Remote Sensing,* 15(14), 2797 - 2808.

Rinehart, R.E., 2004. *RADAR For Meteorologists* ,Rinehart Publications, Nevada, Missouri, 482 p.

Saatchi, S., M. Marlier, R.L. Chazdon, D.B. Clark, A.E. Russell, 2011. Impact of Spatial Variability of Tropical Forest Structure on Radar Estimation of Aboveground Biomass, *Remote Sensing of Environment,* 115(11): 2836 - 2849.

Schuur, T.J., 2003. Polarimetric Radar Page, URL: http://www.cimms.ou.edu/~schuur/dualpol/, National Severe Storms Laboratory, Norman, Oklahoma (last date accessed: 2 January, 2012).

Scipal, K., M. Arcioni, J. Chave, J. Dall, F. Fois, T. LeToan, C. Lin, K. Papathanassiou, S. Quegan, F. Rocca, S. Saatchi, H. Shugart, L. Ulander, M. Williams, 2010. The BIOMASS Mission – An ESA Earth Explorer Candidate to Measure the Biomass of the Earth's Forests, *IEEE International Geoscience and Remote Sensing Symposium 2010,* 25-30 July 2010, Honolulu, Hawaii, pp. 52-55.

Segal, D.B., 1983. SEASAT Synthetic Aperture Radar (SAR) Response to Lowland Vegetation Types in Eastern Maryland and Virginia, *Journal of Geophysical Research,* 88(c3): 1937-1952.

Short, 2010, Radar Polarization, The Remote Sensing Tutorial, http://rst.gsfc.nasa.gov/Sect8/Sect8_5.html, National Aeronautics and Space Administration, Washington, District of Columbia (last date accessed: 2 January, 2012).

Stellingwerf, D.A. and Y.A. Hussin, 1997. *Measurements and Estimations of Forest Stand Parameters Using Remote Sensing*, VSP, Utrecht, Netherlands, 272 p.

Trincado, G., C.L. VanderSchaaf, and H.E. Burkhart, 2006. Regional mixed-effects height-diameter models for loblolly pine (*Pinus taeda L.*) plantations, *European Journal of Forest Research*, 126(2): 253-262.

U.S. Department of Agriculture (USDA), 2001. Rangeland Soil Quality – Infiltration, Soil Quality Information Sheet – 5, URL: http://soils.usda.gov/sqi/management/files/RSQIS5.pdf, U.S. Department of Agriculture, Washington, District of Columbia (last date accessed: 27 October 2011).

Wang, H., K. Ouchi., M. Watanabe, M. Shimada, T. Tadono, A. Rosenqvist, S A. Romshoo, M. Matsuoka, T. Moriyama, and S. Uratsuka, 2006. In Search of the Statistical Properties of High-Resolution Polarimetric SAR Data for the Measurements of Forest Biomass Beyond the RCS Saturation Limits, *IEEE Geoscience and Remote Sensing Letters*, 3(4): 495 - 499.

Whitall, D.R. and H.W. Paerl, 2001. Spatiotemporal Variability of Wet Atmosphere Nitrogen Deposition to the Neuse River Estuary, North Carolina, *Journal of Environmental Quality*, 30(5): 1508 – 1515.

Williams, T.M. and C.A. Gresham, 2006. Biomass accumulation in rapidly growing loblolly pine and sweetgum, *Biomass and Bioenergy*, 30(4): 370-377.

Woudenberg, S.W., B.L. Conkling, B.M. O'Connell, E.B. LaPoint, J.A. Turner, K.L. Waddell, 2010. The Forest Inventory and Analysis Database: Database Description and Users Manual Version 4.0 for Phase 2, URL: http://www.fs.fed.us/rm/pubs/rmrs_gtr245.pdf, US Forest Service, Washington, District of Columbia (last date accessed: 1 December 2011).

Wu, S.T., 1987. Potential Application of Multipolarization SAR for Pine-Plantation Biomass Estimation, *IEEE Transactions on Geoscience and Remote Sensing*, GE-25(3): 403-409.

Wu, S.T. and S.A. Sader, 1987. Multipolarization SAR Data for Surface Feature Delineation and Forest Vegetation Characterization, *IEEE Transactions on Geoscience and Remote Sensing*, GE-25 (1): 67-76.

APPENDICES

Appendix A. Within-Stand Backscatter Intensity Variability Tables

The following tables display summary statistics for each of the loblolly pine sample sites. Type indicates natural (N) or plantation (P) stands. The mean, range, standard deviation (Std Dev), and coefficient of variance (C of V) of backscatter values are provided.

Within-Stand Variation - 3x3 HH

Site	Type	BA_sq_m_ha	Biomass_T_Ha	Mean	Range	Std Dev	C of V
1	N	29.842007	65.93	0.617718	1.109646	0.299869	0.485447
2	N	36.728625	120.02	0.77633	1.045773	0.30183	0.388791
3	N	41.319703	161.36	1.134246	0.92985	0.315169	0.277867
5	P	20.659851	89.54	1.329381	2.244052	0.686932	0.516731
6	P	20.659851	106.6	0.81589	1.144769	0.338364	0.414717
7	P	18.364312	95.02	1.060697	1.13326	0.358042	0.337553
10	P	50.501859	248.12	1.034267	1.396585	0.420219	0.406296
11	P	52.797398	262.27	0.963809	0.829565	0.268933	0.279031
12	P	50.501859	246.54	0.972256	0.73433	0.260476	0.267908
13	N	45.910781	197.06	0.955483	0.597802	0.191303	0.200216
14	N	45.910781	177.25	1.572732	1.688531	0.515654	0.327871
15	N	48.20632	187.02	1.099529	1.027106	0.359244	0.326726
16	N	34.433086	165.39	1.356439	1.515285	0.416188	0.306824
17	N	34.433086	164.6	0.924332	0.587224	0.199628	0.21597
18	P	16.068773	80.44	0.992983	0.941882	0.32497	0.327267
19	P	16.068773	81.66	0.848087	1.039302	0.330558	0.389769
20	P	18.364312	93.48	0.97415	0.982269	0.333594	0.342446
23	N	32.137546	101.75	1.141094	1.430147	0.550541	0.482468
24	P	25.250929	127.3	1.288836	0.990561	0.357514	0.277393
27	N	36.728625	169.48	1.228203	1.450373	0.576476	0.469365
29	N	16.068773	87.21	1.150495	1.721793	0.480709	0.417828
35	P	16.068773	112.73	1.071637	1.198346	0.354417	0.330725
36	P	11.477695	79.33	0.974697	1.276554	0.42571	0.436762
37	P	16.068773	98.83	1.604499	2.076761	0.535075	0.333484

Within-Stand Variation - 3x3 HV

Site	Type	BA_sq_m_ha	Biomass_T_Ha	Mean	Range	Std Dev	C of V
1	N	29.84201	65.93	0.122771	0.203092	0.055034	0.448263
2	N	36.72863	120.02	0.286514	0.413706	0.121566	0.424292
3	N	41.3197	161.36	0.283513	0.398182	0.120399	0.424669
5	P	20.65985	89.54	0.317444	0.550858	0.156559	0.493185
6	P	20.65985	106.6	0.305821	0.35669	0.108853	0.355938
7	P	18.36431	95.02	0.286359	0.199934	0.074818	0.261275
10	P	50.50186	248.12	0.395114	0.403456	0.146756	0.371427
11	P	52.7974	262.27	0.333292	0.291247	0.114181	0.342584
12	P	50.50186	246.54	0.446053	0.458348	0.147174	0.329947
13	N	45.91078	197.06	0.347552	0.145386	0.042701	0.122861
14	N	45.91078	177.25	0.491514	0.373297	0.107654	0.219024
15	N	48.20632	187.02	0.458841	0.434111	0.13426	0.292607
16	N	34.43309	165.39	0.342215	0.334832	0.10593	0.309542
17	N	34.43309	164.6	0.342965	0.277429	0.090348	0.263431
18	P	16.06877	80.44	0.497222	0.569221	0.190374	0.382876
19	P	16.06877	81.66	0.388297	0.631355	0.176309	0.454058
20	P	18.36431	93.48	0.389171	0.380017	0.146984	0.377686
23	N	32.13755	101.75	0.399057	0.430324	0.166059	0.416129
24	P	25.25093	127.3	0.419206	0.601098	0.187888	0.448201
27	N	36.72863	169.48	0.397023	0.470261	0.156959	0.39534
29	N	16.06877	87.21	0.341104	0.398024	0.157304	0.461163
35	P	16.06877	112.73	0.463592	0.686389	0.19635	0.423541
36	P	11.4777	79.33	0.407511	0.722833	0.216604	0.53153
37	P	16.06877	98.83	0.311962	0.265754	0.097943	0.313958

Within-Stand Variation - 3x3 VV							
Site	**Type**	**BA_sq_m_ha**	**Biomass_T_Ha**	**Mean**	**Range**	**Std Dev**	**C of V**
1	N	29.84201	65.93	0.693429	0.734347	0.205533	0.296401
2	N	36.72863	120.02	0.794174	0.945024	0.325504	0.409865
3	N	41.3197	161.36	0.751499	0.711048	0.184054	0.244916
5	P	20.65985	89.54	1.259697	2.649586	0.763849	0.606375
6	P	20.65985	106.6	0.822049	0.863631	0.250163	0.304317
7	P	18.36431	95.02	1.005281	1.090496	0.418285	0.416087
10	P	50.50186	248.12	1.110224	0.634485	0.183252	0.165059
11	P	52.7974	262.27	0.992526	0.836564	0.267951	0.269969
12	P	50.50186	246.54	1.218838	1.014618	0.409341	0.335845
13	N	45.91078	197.06	1.215933	0.884712	0.305651	0.251371
14	N	45.91078	177.25	1.624167	2.278045	0.65627	0.404065
15	N	48.20632	187.02	1.046449	0.877452	0.270473	0.258467
16	N	34.43309	165.39	0.873272	0.925488	0.283365	0.324486
17	N	34.43309	164.6	1.124658	1.109211	0.337545	0.300131
18	P	16.06877	80.44	1.138022	1.229333	0.472448	0.415149
19	P	16.06877	81.66	0.953599	0.942564	0.312968	0.328196
20	P	18.36431	93.48	1.125726	1.040604	0.305133	0.271055
23	N	32.13755	101.75	1.320622	2.114394	0.784085	0.593724
24	P	25.25093	127.3	1.522356	2.114352	0.720312	0.473156
27	N	36.72863	169.48	1.113625	1.114728	0.464296	0.416923
29	N	16.06877	87.21	1.043057	1.646603	0.463403	0.444274
35	P	16.06877	112.73	0.847087	1.27039	0.35207	0.415625
36	P	11.4777	79.33	1.183464	1.199759	0.433418	0.366228
37	P	16.06877	98.83	1.431709	2.065643	0.683063	0.477096

Within-Stand Variability - 5x5 HH							
Site	**Type**	**BA_sq_m_ha**	**Biomass_T_Ha**	**Mean**	**Range**	**Std Dev**	**C of V**
1	N	29.84201	65.93	0.564303	1.159739	0.346534	0.614092
2	N	36.72863	120.02	0.73859	2.494128	0.503442	0.681625
3	N	41.3197	161.36	1.078322	1.539727	0.463802	0.430114
5	P	20.65985	89.54	1.114572	2.25461	0.521245	0.467664
6	P	20.65985	106.6	0.81503	1.311933	0.284613	0.349206
7	P	18.36431	95.02	1.044065	2.019566	0.418317	0.400662
10	P	50.50186	248.12	0.895893	1.547551	0.320017	0.357204
11	P	52.7974	262.27	1.004346	1.052835	0.29755	0.296262
12	P	50.50186	246.54	0.898616	0.851362	0.236974	0.26371
13	N	45.91078	197.06	0.848636	0.764848	0.209159	0.246465
14	N	45.91078	177.25	1.515996	2.029804	0.542478	0.357836
15	N	48.20632	187.02	1.117088	1.669302	0.416455	0.372804
16	N	34.43309	165.39	0.998534	1.8824	0.502743	0.503481
17	N	34.43309	164.6	0.812594	0.590745	0.198327	0.244067
18	P	16.06877	80.44	0.834621	1.060172	0.299772	0.359171
19	P	16.06877	81.66	0.809982	1.064495	0.26466	0.326748
20	P	18.36431	93.48	0.83111	1.332206	0.353064	0.42481
23	N	32.13755	101.75	0.95835	1.585043	0.550009	0.573913
24	P	25.25093	127.3	1.325342	2.33424	0.522878	0.394523
27	N	36.72863	169.48	1.098459	1.578044	0.582047	0.529875
29	N	16.06877	87.21	1.019912	1.939561	0.367146	0.359978
35	P	16.06877	112.73	1.156224	1.629541	0.461787	0.399392
36	P	11.4777	79.33	1.191378	1.879715	0.52659	0.442001
37	P	16.06877	98.83	1.320083	2.245657	0.620754	0.470238

Within-Stand Variability - 5x5 VV							
Site	**Type**	**BA_sq_m_ha**	**Biomass_T_Ha**	**Mean**	**Range**	**Std Dev**	**C of V**
1	N	29.84201	65.93	0.587844	0.92732	0.246437	0.419221
2	N	36.72863	120.02	0.809605	1.642344	0.467229	0.577108
3	N	41.3197	161.36	0.95283	2.210043	0.555465	0.582963
5	P	20.65985	89.54	1.193882	2.745975	0.782695	0.655588
6	P	20.65985	106.6	0.778682	1.013185	0.263069	0.337838
7	P	18.36431	95.02	0.999481	1.729191	0.429235	0.429457
10	P	50.50186	248.12	1.12257	2.316134	0.435302	0.387773
11	P	52.7974	262.27	1.002585	1.631483	0.329401	0.328551
12	P	50.50186	246.54	1.101416	1.470037	0.414195	0.376057
13	N	45.91078	197.06	1.089384	1.905886	0.447325	0.410622
14	N	45.91078	177.25	1.533878	2.494404	0.606582	0.395456
15	N	48.20632	187.02	1.006413	0.890241	0.297403	0.295508
16	N	34.43309	165.39	0.986552	1.288988	0.387064	0.392341
17	N	34.43309	164.6	1.13807	1.161207	0.330039	0.289999
18	P	16.06877	80.44	1.038674	1.234845	0.381261	0.367065
19	P	16.06877	81.66	0.939028	1.00309	0.295497	0.314684
20	P	18.36431	93.48	1.033127	1.093276	0.342235	0.331261
23	N	32.13755	101.75	1.100638	2.2783	0.691002	0.62782
24	P	25.25093	127.3	1.278004	2.277523	0.541059	0.423363
27	N	36.72863	169.48	1.034937	2.132659	0.491399	0.47481
29	N	16.06877	87.21	0.883281	1.827409	0.353152	0.399818
35	P	16.06877	112.73	0.986529	1.765757	0.495797	0.502567
36	P	11.4777	79.33	1.198242	2.200845	0.590382	0.492707
37	P	16.06877	98.83	1.1075	2.242282	0.565779	0.510862

Within-Stand Variability - 5x5 HV							
Site	**Type**	**BA_sq_m_ha**	**Biomass_T_Ha**	**Mean**	**Range**	**Std Dev**	**C of V**
1	N	29.84201	65.93	0.12682	0.225319	0.05783	0.456
2	N	36.72863	120.02	0.256398	0.451195	0.129931	0.506757
3	N	41.3197	161.36	0.344174	0.908795	0.24009	0.697582
5	P	20.65985	89.54	0.343727	0.550858	0.154197	0.448603
6	P	20.65985	106.6	0.317212	0.4776	0.141178	0.445059
7	P	18.36431	95.02	0.312747	0.500728	0.10425	0.333337
10	P	50.50186	248.12	0.370451	0.427367	0.123032	0.332113
11	P	52.7974	262.27	0.440172	0.702033	0.176429	0.400819
12	P	50.50186	246.54	0.441383	0.517948	0.134757	0.305306
13	N	45.91078	197.06	0.391237	0.383219	0.107665	0.27519
14	N	45.91078	177.25	0.451574	0.542677	0.132269	0.292907
15	N	48.20632	187.02	0.440832	0.485931	0.125985	0.285788
16	N	34.43309	165.39	0.34193	0.544229	0.158491	0.46352
17	N	34.43309	164.6	0.328671	0.50485	0.118579	0.360783
18	P	16.06877	80.44	0.435602	0.65382	0.192453	0.44181
19	P	16.06877	81.66	0.415431	0.631355	0.150698	0.36275
20	P	18.36431	93.48	0.309529	0.432419	0.145477	0.469996
23	N	32.13755	101.75	0.333409	0.471243	0.155906	0.467611
24	P	25.25093	127.3	0.428633	0.713775	0.199025	0.464325
27	N	36.72863	169.48	0.348327	0.477697	0.161585	0.463891
29	N	16.06877	87.21	0.332532	0.398024	0.124053	0.373054
35	P	16.06877	112.73	0.436753	0.778767	0.182471	0.41779
36	P	11.4777	79.33	0.399627	0.879821	0.214303	0.536258
37	P	16.06877	98.83	0.268438	0.562372	0.124858	0.465129

Within-Stand Variability - 7x7 HH							
Site	**Type**	**BA_sq_m_ha**	**Biomass_T_Ha**	**Mean**	**Range**	**Std Dev**	**C of V**
1	N	29.84201	65.93	0.715836	0.599255	0.597056	0.834068
2	N	36.72863	120.02	0.990026	0.60642	0.640719	0.647174
3	N	41.3197	161.36	0.964613	0.726764	0.473356	0.490721
5	P	20.65985	89.54	1.059728	0.247654	0.437453	0.412797
6	P	20.65985	106.6	0.778246	0.452476	0.381862	0.490669
7	P	18.36431	95.02	1.002084	0.336411	0.438937	0.438024
10	P	50.50186	248.12	0.911235	0.521382	0.316976	0.347854
11	P	52.7974	262.27	0.921134	0.484757	0.277595	0.301363
12	P	50.50186	246.54	0.898822	0.317088	0.223036	0.248143
13	N	45.91078	197.06	0.837959	0.324652	0.226894	0.27077
14	N	45.91078	177.25	1.655091	0.338517	0.748146	0.452027
15	N	48.20632	187.02	0.967657	0.666635	0.426256	0.440503
16	N	34.43309	165.39	0.805476	0.460049	0.504645	0.626517
17	N	34.43309	164.6	0.775959	0.348001	0.244896	0.315604
18	P	16.06877	80.44	0.912159	0.527414	0.347152	0.380582
19	P	16.06877	81.66	0.762309	0.406066	0.258382	0.338946
20	P	18.36431	93.48	0.828946	0.546924	0.336747	0.406235
23	N	32.13755	101.75	0.972503	0.255741	0.568384	0.584455
24	P	25.25093	127.3	1.289365	0.690176	0.466384	0.361716
27	N	36.72863	169.48	1.073956	0.796903	0.640526	0.596417
29	N	16.06877	87.21	1.124118	0.30251	0.527095	0.468897
35	P	16.06877	112.73	1.193311	0.622188	0.628099	0.52635
36	P	11.4777	79.33	1.16422	0.627415	0.509406	0.437551
37	P	16.06877	98.83	1.149424	0.393127	0.646283	0.562267

Within-Stand Variability - 7x7 VV							
Site	**Type**	**BA_sq_m_ha**	**Biomass_T_Ha**	**Mean**	**Range**	**Std Dev**	**C of V**
1	N	29.84201	65.93	0.689014	1.900138	0.449737	0.652726
2	N	36.72863	120.02	1.022401	1.928391	0.505863	0.494779
3	N	41.3197	161.36	0.932328	2.287683	0.535274	0.574126
5	P	20.65985	89.54	1.093283	2.782585	0.631442	0.577565
6	P	20.65985	106.6	0.754536	1.498997	0.356081	0.47192
7	P	18.36431	95.02	1.010276	1.911394	0.410948	0.406768
10	P	50.50186	248.12	1.142301	2.316134	0.353511	0.309473
11	P	52.7974	262.27	1.072275	1.631483	0.353911	0.330056
12	P	50.50186	246.54	1.032181	1.561795	0.39745	0.385058
13	N	45.91078	197.06	1.019091	2.196898	0.408905	0.401245
14	N	45.91078	177.25	1.597929	3.727925	0.72793	0.455546
15	N	48.20632	187.02	0.980133	1.602737	0.373351	0.380919
16	N	34.43309	165.39	0.866274	1.698024	0.455285	0.525567
17	N	34.43309	164.6	1.082121	1.161207	0.331622	0.306456
18	P	16.06877	80.44	1.106207	1.493758	0.422507	0.381942
19	P	16.06877	81.66	0.892852	1.098358	0.284578	0.31873
20	P	18.36431	93.48	1.037153	2.178142	0.41218	0.397414
23	N	32.13755	101.75	1.102478	2.2783	0.612217	0.55531
24	P	25.25093	127.3	1.10673	2.38939	0.508971	0.459887
27	N	36.72863	169.48	1.015679	2.132659	0.471536	0.464257
29	N	16.06877	87.21	1.025459	2.1618	0.459635	0.448224
35	P	16.06877	112.73	1.163245	3.322285	0.702968	0.604317
36	P	11.4777	79.33	1.272821	2.478369	0.580419	0.45601
37	P	16.06877	98.83	0.923536	2.274155	0.529938	0.573814

Within-Stand Variability - 7x7 HV							
Site	**Type**	**BA_sq_m_ha**	**Biomass_T_Ha**	**Mean**	**Range**	**Std Dev**	**C of V**
1	N	29.84201	65.93	0.155298	0.63205	0.119661	0.770521
2	N	36.72863	120.02	0.317781	0.698279	0.17075	0.537321
3	N	41.3197	161.36	0.300209	0.908795	0.194683	0.648494
5	P	20.65985	89.54	0.340271	0.550858	0.135483	0.398163
6	P	20.65985	106.6	0.287919	0.564615	0.147302	0.511609
7	P	18.36431	95.02	0.328965	0.566632	0.132612	0.403118
10	P	50.50186	248.12	0.382912	0.735843	0.144538	0.377471
11	P	52.7974	262.27	0.445499	0.702033	0.139904	0.31404
12	P	50.50186	246.54	0.435515	0.619366	0.122485	0.281242
13	N	45.91078	197.06	0.382451	0.588333	0.142694	0.373104
14	N	45.91078	177.25	0.48792	0.652717	0.181075	0.371116
15	N	48.20632	187.02	0.389703	0.842386	0.157318	0.403688
16	N	34.43309	165.39	0.290708	0.544551	0.170991	0.588186
17	N	34.43309	164.6	0.354609	0.529979	0.137616	0.388079
18	P	16.06877	80.44	0.419887	0.815463	0.190579	0.453882
19	P	16.06877	81.66	0.389485	0.660187	0.153272	0.393525
20	P	18.36431	93.48	0.327769	0.642172	0.143047	0.436425
23	N	32.13755	101.75	0.32142	0.506812	0.156448	0.48674
24	P	25.25093	127.3	0.415911	1.035103	0.216247	0.519937
27	N	36.72863	169.48	0.354123	0.890434	0.175313	0.495062
29	N	16.06877	87.21	0.365968	0.693576	0.145684	0.398078
35	P	16.06877	112.73	0.413729	0.857073	0.200215	0.483927
36	P	11.4777	79.33	0.396564	0.879821	0.197186	0.497237
37	P	16.06877	98.83	0.245372	0.562389	0.115645	0.471303

Appendix B. Within-Stand Backscatter Intensity Variance / Forest Metrics Tables

The following tables display correlation between within stand variance of backscatter intensity against biomass and basal area for each window size and polarization combination.

R^2 Value (Within Stand Coefficient of Variation vs. Basal Area)			
	HH	**VV**	**HV**
3x3	0.1296	0.2247	0.2426
5x5	0.0363	0.028	0.0965
7x7	0.0411	0.0817	0.0557

R^2 Value (Within Stand Coefficient of Variation vs. Biomass)			
	HH	**VV**	**HV**
3x3	0.25	0.2679	0.2519
5x5	0.2018	0.0899	0.1439
7x7	0.2104	0.2163	0.2187

The following tables display the correlation between within stand variance of backscatter intensity against biomass area for each window size and polarization combination based on whether the sites are natural or plantation.

Natural
R^2 Value (Within Stand Coefficient of Variation vs. Biomass)

	HH	VV	HV
3x3	0.5274	0.2227	0.6085
5x5	0.3361	0.1237	0.0903
7x7	0.4466	0.3655	0.2532

Plantation
R^2 Value (Within Stand Coefficient of Variation vs. Biomass)

	HH	VV	HV
3x3	0.1635	0.3021	0.1222
5x5	0.4444	0.0997	0.3346
7x7	0.3901	0.2198	0.5042

Appendix C. Model Expressions

Expressions used to extract values from UAVSAR raster in Imagine models. UAVSAR dataset, sample sites shapefile, and a matrix specifying window size are all input into an EITHER function containing these expressions.

EITHER (FOCAL MIN ($n1_uavsar_sub, $n3_Custom_Float)) IF ($n2_neuse_sites021511) OR 0 OTHERWISE

EITHER (FOCAL MAX ($n1_uavsar_sub, $n3_Custom_Float)) IF ($n2_neuse_sites021511) OR 0 OTHERWISE

EITHER (FOCAL MEAN ($n1_uavsar_sub, $n3_Custom_Float)) IF ($n2_neuse_sites021511) OR 0 OTHERWISE